

Nanoscale Electromagnetic Compatibility: Quantum Coupling and Matching in Nanocircuits

Gregory Y. Slepyan, Amir Boag, *Fellow, IEEE*, Vladimir Mordachev, *Member, IEEE*, Eugene Sinkevich, Sergey Maksimenko, Polina Kuzhir, Giovanni Miano, Mikhail. E. Portnoi, and Antonio Maffucci, *Senior Member, IEEE*

Abstract—The paper investigates two typical electromagnetic compatibility (EMC) problems, namely, coupling and matching in nanoscale circuits composed of nano-interconnects and quantum devices in entangled state. Nano-interconnects under consideration are implemented by using carbon nanotubes or metallic nanowires, while quantum devices - by semiconductor quantum dots. Equivalent circuits of such nanocircuits contain additional elements arising at nanoscale due to quantum effects. As a result, the notions of coupling and impedance matching are reconsidered. Two examples are studied: in the first one, electromagnetically coupled nanowires are connected to classical lumped devices; in the second one, electromagnetically uncoupled transmission lines are terminated on quantum devices in entangled states. In both circuits the EMC features qualitatively and quantitatively differ from their classical analogs. In the second example, we demonstrate the existence of quantum coupling, due to the entanglement, which exists in spite of the absence of classical electromagnetic coupling. The entanglement also modifies the matching condition introducing a dependence of the optimal value of load impedance on the line length.

Index Terms — Electromagnetic compatibility, kinetic inductance, nano-circuits, nano-electromagnetism, quantum devices, quantum entanglement.

I. INTRODUCTION

TODAY'S achievements of nanoelectronics allow utilization and manipulation of small collections of atoms and molecules, such as semiconductor heterostructures, quantum wells, quantum wires and quantum dots [1-3], different forms of nanocarbon (spherical fullerenes, graphene, carbon nanotubes [4-7]), noble metal nanowires [8], organic macromolecules and organic polymers [9]. The increasingly intensive penetration of nanotechnologies lead to the birth of the so-called “nanoelectromagnetism” [10-11], a novel branch of applied science related to the interaction of electromagnetic

radiation with quantum mechanical low-dimensional systems.

One of the crucial aspects of electromagnetism for electronic devices and systems is related to their electromagnetic compatibility, i.e., of their ability to operate successfully, with controlled levels of emissions and with a suitable degree of robustness to unwanted electromagnetic couplings via various mechanisms of interference [12-14].

However, with the transition of electronics to nanoscale new physical phenomena as well as new materials' properties need to be studied. Quantum effects, such as: discrete energy spectrum of charge carriers, existence of phonons, ballistic transport and tunneling, many-body correlations, interface effects, and so on, manifest themselves jointly with classical electromagnetic interactions [15-16]. As a result, the classical design based on the phenomenological separate analysis of physical properties of electric circuit elements and functional properties of devices and systems becomes invalid with respect to nanoelectronics. These considerations lead to the conclusion that the “classical” EMC, completely based on macroscopic electrodynamics, must be deeply revised starting from the basic concepts and opening the era of “nanoEMC” [17-19].

For instance, the classical scaling rules used to design integrated circuits (ICs) and to implement EMC solutions are based on the macroscopic behavior of the electrical parameters, such as inductances and capacitances. However, the quantum terms appearing in the models of nanoelectronics change the dependence of such electrical parameters on frequency, geometry and temperature. Consequently, the classical EMC concepts like coupling, shielding, and matching, should be reconsidered, along with the classical solutions to such issues. In other words, nanoEMC poses new challenges in modeling devices and systems, in establishing new design rules and in assessing reliable characterization procedures.

Manuscript received, 2015. This work was supported in part by FP7-PEOPLE-2013-IRSES-612285 CANTOR.

G. Slepyan and Amir Boag are with the School of Electrical Engineering, Tel-Aviv University, Tel-Aviv, Israel (e-mail: gregory_slepyan@yahoo.com, boag@eng.tau.ac.il)

V. Mordachev and E. Sinkevich are with the EMC R&D laboratory of Belarusian State University of Informatics and Radioelectronics, Minsk, Belarus (emc@bsuir.by).

S. Maksimenko and P. Kuzhir are with the Research Institute for Nuclear Problems of Belarusian State University, Minsk, Belarus (sergey.maksimenko@gmail.com, polina.kuzhir@gmail.com).

G. Miano is with the Department of Electrical Engineering and Information Technology, University of Naples Federico II, Naples, Italy (miano@unina.it).

M. E. Portnoi is with the School of Physics, University of Exeter, Exeter, UK (M.E.Portnoi@exeter.ac.uk)

A. Maffucci is with the Department of Electrical and Information Engineering, University of Cassino and Southern Lazio, Cassino, Italy and with INFN-LNF Frascati, Italy (maffucci@unicas.it).

NanoEMC modeling assumes the self-consistent solution of Maxwell's equations with the quantum transport equations for charge carriers. Transition from the macroscopic to the atomic scale can be performed via either of the three distinct approaches to electron transport modeling: classical, semi-classical, and quantum. Many works were devoted to this topic, investigating nanomaterials for EMC applications like shielding [20-21], modeling the interactions between EM fields and nano-structures [22-23], and modeling nano-interconnects [24-29].

The classical approach, with the most limited validity area, is the simplest one. For example, Drude model of conductivity in metals [16], considers the conducting electron as a classical particle, which moves in the electric field while encountering inelastic collisions with a randomly vibrating ion lattice.

The semi-classical approach is based on the concept of a particle ensemble behaving as a non-ideal gas with quantum effects taken into account by replacing the real particle mass by the corresponding effective value [15-16]. In these models, electrons are unable to tunnel through barriers. In collision events, the electrons' scattering is inelastic, thus the kinetic energy of incident particles is not conserved. The transmission line (TL) model for carbon nanotube (CNT) interconnects presented in [28-29] may be noted as an example of such a semi-classical approach.

On the contrary, at the molecular or atomic scale a quantum approach is needed, since the transport is governed by the wave-like behavior of the electrons. Thus, unwanted interactions between elements exist both due to electromagnetic coupling and quantum phenomena, such as tunneling, spin-orbit interaction, and various many-body effects including dipole-dipole and spin-spin interactions. As a result, appears the entanglement of quantum states, which produces the long-living and long-distance correlations of quantum origin in electric circuits [16]. For their description the complete Maxwell-Schrödinger model is necessary. One of the most convenient forms of it is based on the concept of generalized susceptibilities (Kubo-approach) [16].

This paper discusses the concepts of *coupling* and *matching* in a nanoscale signaling system composed of nanowires connecting quantum devices in the entangled states. The interest in this type of systems from the EMC point of view stems mainly from their potential as digital elements for quantum computing and quantum informatics [1]. In particular, the paper compares predictions of the conventional EMC-theory with those of nanoEMC taking into account the coupling of quantum nature, due to the entanglement.

The paper is organized as follows. Section II is devoted to the modeling. First, the TL model for nano-interconnects based on metal nanowires (NWs) or carbon nanotubes (CNTs) is briefly recalled. Then, an equivalent lumped model to describe a pair of quantum devices in entangled state is proposed. Section III deals with the analysis of two complementary case-studies: the first one refers to a nano-interconnect with a crosstalk noise induced by an unwanted electromagnetic coupling. The second proposes two uncoupled nanowires terminated on two quantum dots in the entangled state. The summary and conclusive remarks are given in Section IV.

II. MODELING A NANOSCALE SIGNALING SYSTEM

In this paper we analyze the behavior of signaling nanocircuits composed of quantum devices connected by nanowires, which play a role of transmission lines. Section II.A summarizes the quasi-classical model of transport in nanowires made of metals or carbon nanotubes, presented in [28-29] and [32], while Section II.B proposes an equivalent lumped model of the quantum devices in the entangled state, in the framework of the circuit theory.

A. Modeling nanoscale interconnects

The considered nano-interconnect (Fig.1) is based on the two signal lines suspended in air above a perfectly conducting ground. The interconnect length is assumed infinite in the z -direction. This model adequately describes a real interconnect if the diameters of the signal lines are much smaller than their lengths (typically, at least an order of magnitude). The conducting material for the signal lines may either be a metallic NW or a CNT. The wire diameter is assumed to be large enough (at least 1 nm) for having a local crystal structure of the wire, which allows the using of *semi-classical transport model*. For assumed ratio between diameter and length, the conducting nanowire can be regarded as a one-dimensional (1-D) material, with the charge transport characterized by two quantum-confined directions and single one unconfined.

The operating frequencies range is from zero up to some THz, so that:

- (i) the cross section diameter D of both nanowires is electrically small;
- (ii) the manifestations of transverse currents in the nanowires may be neglected;
- (iii) only the intraband transitions in the particle movement are taken into account.

Since the conducting electrons are laterally quantum confined, they occupy the narrow energy subbands, instead of the ordinary wide bands found in the bulk materials. Along the longitudinal axis, the lattice exhibits translational symmetry and is long enough to consider the longitudinal electron wave-number as a continuous value. Such type of energy spectrum may be evaluated by means of the *tight-binding approximation* (e.g., CNTs, [30]), or first principle calculations (e.g., copper NWs, [31]).

In the semi-classical approximation, the electrons are considered as a 1-D gas described by the Boltzmann transport equation. The quantum nature of the conductive electrons is accounted via a non-parabolic dispersive law [28-29].

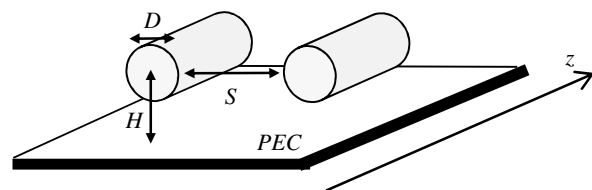


Figure 1. Reference geometry for the nano-interconnect: to signal lines above a Perfect Electric Conducting (PEC) ground.

In the momentum domain the traveling wave can be presented as $\exp\{i(\alpha z - \beta z)\}$, where ω is the radian frequency and β is the wavenumber. By solving the transport equation in such a domain, we get the following expression for the longitudinal component of the current density, \hat{J}_z , [28-29]:

$$\hat{J}_z(\beta, \omega) = \hat{\sigma}_{zz}(\beta, \omega) \hat{E}_z(\beta, \omega), \quad (1)$$

where \hat{E}_z is the longitudinal component of the electric field, and $\hat{\sigma}_{zz}$ is the longitudinal conductivity. The latter can be evaluated as the sum of all the contributions of the subbands:

$$\hat{\sigma}_{zz}(\beta, \omega) = \sum_{\mu=1}^N \hat{\sigma}_{\mu}. \quad (2)$$

Here the number N refers to the subbands that significantly contribute to the conduction, namely those for which the energy gap with respect to the Fermi level is small enough, usually $|E_{\mu} - E_F| \leq 5k_B T$, where E_F and E_{μ} are, respectively, the energies of the Fermi level and of the μ -th energy subband (in eV), T is the absolute temperature and k_B the Boltzmann constant (in eV/K). Assuming the collision frequency ν to be constant for all the subbands close to the Fermi level, it results:

$$\hat{\sigma}_{zz}(\beta, \omega) \equiv -i \frac{2e^2 v_F}{\pi X \hbar} \frac{1}{\omega - i\nu} M \left[1 - \xi(\omega) \left(\frac{v_F \beta}{\omega - i\nu} \right)^2 \right]^{-1}, \quad (3)$$

where \hbar is the reduced Planck constant, v_F is the Fermi velocity, M is the equivalent number of conducting channels [28], and the quantities X and $\xi(\omega)$ depend on the material used as signal trace. For the case of CNT, the quantity X is its circumference, and [32]:

$$X = \pi D, \quad \xi(\omega) = 1, \quad (4)$$

while for a nanowire, X is its cross section S_W , and [33]:

$$X = S_W = \frac{\pi}{4} D^2, \quad \xi(\omega) = \frac{1}{3} \frac{1 + 1.8i\omega/\nu}{1 + i\omega/\nu}. \quad (5)$$

By combining (3) and (1), we get a *generalized Ohm's law*:

$$\left[1 - \psi(\omega) \beta^2 \right] \hat{J}_z(\beta, \omega) = \frac{\sigma_0}{1 + i\omega/\nu} \hat{E}_z(\beta, \omega), \quad (6)$$

where

$$\psi(\omega) = \frac{\xi(\omega) v_F^2}{\nu^2 (1 + i\omega/\nu)^2}, \quad (7)$$

$$\sigma_0 = \frac{2v_F M}{\nu R_0 X}. \quad (8)$$

and $R_0 = \pi \hbar / e^2 = 12.9 \text{ k}\Omega$ is the quantum resistance. Note that the number of conducting channels M strongly depends on the chirality, size and temperature [34]-[36].

If we assume an uniform distribution of the current, *i.e.*, $I(z, \omega) = J(z, \omega) X$, we can multiply both parts of (6) by X and rewrite it in spatial-frequency domain (using $\beta \rightarrow -\partial^2 / \partial z^2$):

$$I(z, \omega) + \psi(\omega) \frac{\partial^2 I(z, \omega)}{\partial z^2} = \frac{\sigma_0 X}{1 + i\omega/\nu} E_z(z, \omega). \quad (9)$$

The second term on the left hand side introduces a spatial and frequency dispersion, whereas the coefficient of the electric field introduces a frequency dispersion.

We assume the electromagnetic field to be low enough for using the linear approximation with respect to it (namely for voltage values, $V < k_B T / e$). Thus, it is possible to derive a simple linear TL model for the nano-interconnect schemes in Figure 1 (*e.g.*, [28], [29], and [32]) by coupling (9) with Maxwell's equations. Assuming a single line (one wire above the ground), we would have the TL equations:

$$-\frac{dV}{dz} = (R_{TL} + i\omega L_{TL})I, \quad -\frac{dI}{dz} = i\omega C_{TL}V, \quad (10)$$

where the per-unit-length (p.u.l.) resistance, inductance and capacitance would be given by:

$$R_{TL} = \frac{\nu L_k}{\Theta(\omega)}, \quad L_{TL} = \frac{L_k + L_M}{\Theta(\omega)}, \quad C_{TL} = C_E, \quad (11)$$

where L_M and C_E are the p.u.l. magnetic inductance and electrostatic capacitance, respectively, and

$$\Theta(\omega) = 1 + \frac{C_E}{C_q} \frac{\xi(\omega)}{1 - i\nu/\omega}, \quad (12)$$

$$L_k = \frac{1}{\nu \sigma_0 X} = \frac{R_0}{2\nu_F M}, \quad C_q = \frac{1}{L_k \nu_F^2} = \frac{2M}{R_0 \nu_F}. \quad (13)$$

In (11)-(13) appear two novel terms with respect to the ordinary macroscopic TL-equations: the p.u.l. *kinetic inductance* L_k , related to the mass inertia of the conduction electrons, and the p.u.l. *quantum capacitance* C_q , related to the quantum pressure arising from the zero-point energy of such electrons.

In spite of their different physical meaning, the *generalized* TL model with parameters (11)-(12), to be valid for CNT lines and metallic NWs, is consistent with the classical TL model for a macroscopic line. To show it, we assume the simple case of a copper wire above the ground, with $D = 400 \text{ nm}$, and $H = 2D$ (see Fig.1). For copper NWs the number of channels M at room temperature may be calculated by $M \approx aS_W + b$, where $a = 0.111(\text{nm})^2$, and $b = 3.036$ (see [31], eq.(4)). In this case it is $M \approx 1.4 \cdot 10^4$. For such a case, it is $\Theta \approx 1$ and $L_k \ll L_M$, and so (11), (12) yield the classical TL parameters: $R_{TL} = 1/(\sigma_0 S_w)$, $L_{TL} = L_M$, $C_{TL} = C_E$.

Here we meet an important difference between macroscopic and nanoscale TLs. For macroscopic TLs the working mode is the Transverse ElectroMagnetic (TEM) wave, with propagation velocity $c = 1/\sqrt{LC}$. The working mode in nano-TLs is a surface wave with rather large longitudinal component, thus from (13) we obtain $v_F = 1/\sqrt{L_k C_q}$. Such coupling condition between linear electric parameters should be taken into account in EMC-applications at nanoscale.

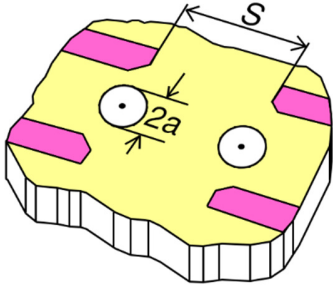


Figure 2. Two quantum-dots interacting with two nano-interconnects.

The TL model presented above have been extended for multiconductor transmission lines (MTLs), where the currents and voltages are presented by vectors, while p.u.l. parameters become a matrices. For operating frequencies up to THz range, it is possible to neglect both the tunneling and the overlap of electronic states in adjacent CNTs or NWs (e.g., [37]). In this case, the kinetic and quantum terms are presented only by the on-diagonal elements of the parameter matrices, while the off-diagonal terms are mainly related to the mutual magnetic inductances and electrostatic capacitances. In other words, only electromagnetic coupling is considered. Finally, the circuit model should be completed by adding lumped terminal resistances, which account for the contact effects.

B. Modeling quantum devices

A challenge for nano-EMC is the study of large (multi-element) quantum digital systems, with dramatically enhanced level of integration. As shortly mentioned in the introduction, quantum computing has been proposed as a new paradigm for information transport, storage and processing, promising a dramatic improvement of device integration and computational performance [38]-[39]. Although a technology for quantum computing is still far from being defined and assessed, the recent literature provides many types of physical systems considered as candidates for basic digital elements of quantum origin. For instance, a possible way to implement the so-called *qubits*, at the basis for quantum computing, is given by the using of quantum dots, coupled via the phenomenon known as *quantum entanglement* [39]-[41]. On the other hand, entanglement is able to manifest itself in the creation of parasitic couplings, unwanted from the EMC point of view. Therefore, it is of interest to introduce -simple models for such quantum devices in the frame of the circuit theory. Here we propose an equivalent two-port lumped model for the device depicted in Fig.2, where a pair of quantum dots (QDs) is placed close to the terminations of two interconnects. Quantum devices show energy spectrum for operated steady states, characterized by wavefunctions localized in a finite spatial area via high potential barriers. The confinement region is approximately given by $A_{eff} \approx 4a^2$, where a is the radius of the QD (or the Bohr radius if the device is a single atom).

We consider a quantum device characterized by two energy states: in this case only one type of transition may be resonant with an external EM-field. Thus, we assume such a field to be monochromatic with frequency approximately equal to the

transition frequency. In addition, we assume that the dimension of the confinement size $2a$ is electrically small at the given frequency, thus the single quantum device may be modeled as a one-port lumped element. We indicate with $V(t)$ and $I(t)$ the voltage and the current intensity of the one-port element. Following [42-43], the device equivalent impedance may be expressed in term of the quantum polarizability, $\alpha(\omega)$, as:

$$Z_L(\omega) = \frac{V}{I} = \frac{i}{\alpha(\omega)\omega} A_{eff}, \quad (14)$$

where, following the Kubo approach [44], it is:

$$\alpha(\omega) = \frac{1}{\hbar} \frac{2\mu^2 \omega_0}{\omega_0^2 - \omega^2 + i\omega\gamma}. \quad (15)$$

In (14)-(15), ω_0 is the frequency of quantum transition between the two stationary states, μ is the dipole moment of the transition, and γ is the spontaneous emission decay.

One of the possible quantum coupling mechanism between the two lumped devices, for instance, exists via dipole-dipole interactions (another coupling mechanism is spin-spin interaction, etc.) [45]. As a consequence, the original two-level energy spectra of the uncoupled quantum devices are transformed now into a one-piece four-level one. In this case, two intermediate levels correspond to the so-called *entangled states* [39]: although only one quantum device is excited, this excitation is distributed with the same probability between both devices, due to quantum correlations [39]. It is necessary to distinguish between symmetric (*superradiant*) and anti-symmetric (*subradiant*) states, which are characterized by different values of transition energies and emission decays [39].

The characteristic of the two-ports representing the pair of quantum devices in the entangled states may be again found by using the Kubo approach [44]. For the symmetric state we have

$$\mathbf{I}(\omega) = \mathbf{Y}(\omega)\mathbf{V}(\omega) = \frac{1}{2Z_L(\omega)} \begin{bmatrix} 1 & 1 \\ 1 & 1 \end{bmatrix} \mathbf{V}(\omega). \quad (16)$$

where $\mathbf{V} = [V_1, V_2]^T$ and $\mathbf{I} = [I_1, I_2]^T$ are the voltages and currents at the two ports, whereas $\mathbf{Y}(\omega)$ is the matrix of equivalent conductivity, and Z_L is given by (14).

III. COUPLING AND MATCHING AT NANOSCALE

In this Section we discuss the concepts of coupling and matching, referring to the simple two-channel signaling system in Fig.3. In order to study the coupling, a typical condition is given by switching on only one driver (for instance which connected to line 1) and evaluating the induced voltages at the near and far end of the other line (line 2), usually normalized to the driver voltage. As for the matching, we will discuss the behavior of the reflection coefficient at the load section.

Here we discuss two complementary cases: (i) two electromagnetically coupled nanowires terminated with two classical uncoupled loads; (ii) two uncoupled ideal transmission lines with quantum devices in entangled states.

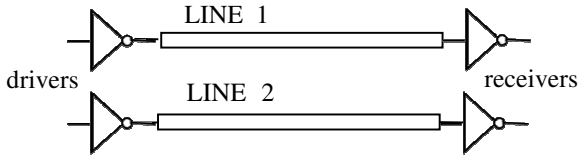


Figure 3. Schematic of a two-channels signaling system.

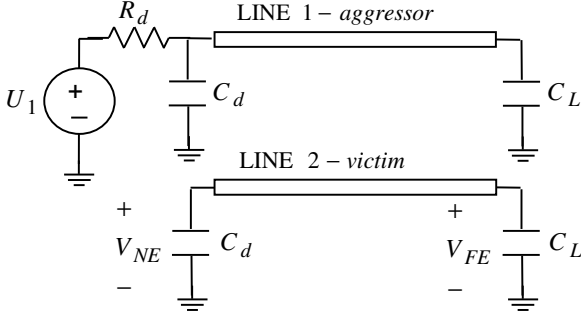


Figure 4. Schematic of a two-line signaling system for crosstalk analysis.

A. Electromagnetically coupled nano-interconnects

In this subsection we consider for crosstalk analysis [46] the MTL in Fig.1, used as a two-channel line in the circuit shown in Fig.4. The drivers and receivers are modeled as real voltage sources and capacitors, respectively.

In macroscale modeling, the crosstalk voltages at the near and far ends of electrically short lines are simply given by [46]:

$$\frac{V_{NE}(\omega)}{U_1(\omega)} = i\omega l(K^{cap} C_m + K^{ind} L_m), \quad (17)$$

$$\frac{V_{FE}(\omega)}{U_1(\omega)} = i\omega l(K^{cap} C_m - K^{ind} L_m), \quad (18)$$

where l is the line length, C_m and L_m are the p.u.l. mutual capacitance and inductance of the line, and K are coupling coefficients related to the terminal impedances. The subscripts NE, FE relate to near-end and far-end voltages, whereas the superscripts cap, ind correspond to capacitance and inductance.

In the wide-separation approximation, the self and mutual terms of the inductance matrix \mathbf{L} for the MTL in Fig.1 are [46]:

$$L_s = \frac{\mu}{2\pi} \ln\left(\frac{2H}{D/2}\right), \quad L_m = \frac{\mu}{4\pi} \ln\left(1 + 4\frac{H^2}{S^2}\right), \quad (19)$$

whereas the p.u.l. capacitance may be evaluated by $\mathbf{C} = \mu\epsilon\mathbf{L}^{-1}$.

We start from a given set of values for the geometrical parameters D, H, S , and l , that provide crosstalk voltages (17) and (18) satisfactorily low for the considered frequencies and loads. In classical applications, this happens, for instance, by following the so-called “ $3W$ spacing rule”, i.e. by assuming the edge-to-edge distance between the signal traces (in this case, S) to be equal to 3 times the trace width W (here replaced by the diameter D). This is a common compromise between acceptable

routing density and crosstalk [14]. We can define a scaling rule reducing the dimensions by the same factor x :

$$D' = Dx, S' = Sx, H' = Hx. \quad (20)$$

After the scaling (20), the crosstalk noise is left unvaried, since the matrices \mathbf{C} and \mathbf{L} do not change, according to (19). If we scale down also the line length l , then the crosstalk noise is proportionally reduced. This simple scaling rule may be rigorously used for lossless lines, and is approximately true for lossy lines too, if the internal inductance can be neglected.

The same behavior may be still found after removing the hypothesis of electrically short lines, hence evaluating the noise voltages as solution of a TL problem. Figure 5 shows the amplitude of the far-end crosstalk voltage, obtained for a classical TL model (pair of copper wires), assuming for parameters defined in Fig.1 the values $D=0.4\text{mm}, H=D, S=3D$, and $l=10\text{mm}$. For the loads shown in Fig.4 we take $C_L = C_D = 1\text{pF}$ and $R_D = 80\Omega$. The result obtained by using (20) with a factor $x = 10$ is the same, since the two curves coincides. The crosstalk noise shows a peak dependent on the value C_L , and shifts to higher frequencies as C_L decreases. In addition, the solution exhibits the typical TL resonances for $\beta l = n\pi$. The line length shortening reduces the level of crosstalk and shifts mentioned resonances to higher frequencies, enlarging the frequency range with negligible level of noise.

We now study the same problem for the nanoscale TL-model (interconnect based on two CNTs). Geometry of the problem again corresponds to Fig.1. We consider either multi-wall CNT of diameter $D = 20\text{nm}$, and metallic single-wall CNT, with $D = 2\text{nm}$. For other parameters, the chosen values are $H = D, S = 3D, l=0.1\text{mm}$. The interconnect is used in a circuit like that in Fig.4, with $C_L = C_D = 0.1\text{pF}$ and $R_D = 3\text{k}\Omega$. To take into account the contact resistance, an additional lumped resistor of $0.5R_0/M$ is added at each termination. The far-end crosstalk noise is reported in Fig.6, considering again the cases when C_L or D are reduced by a factor of 10.

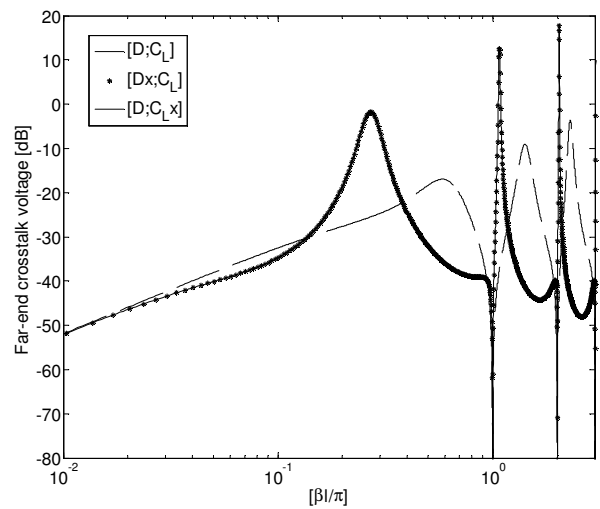


Figure 5. Far-end crosstalk noise for the circuit in Fig.4, assuming a classical TL model (two copper lines), after scaling the wire diameter D and/or the load capacitance C_L by a factor x .

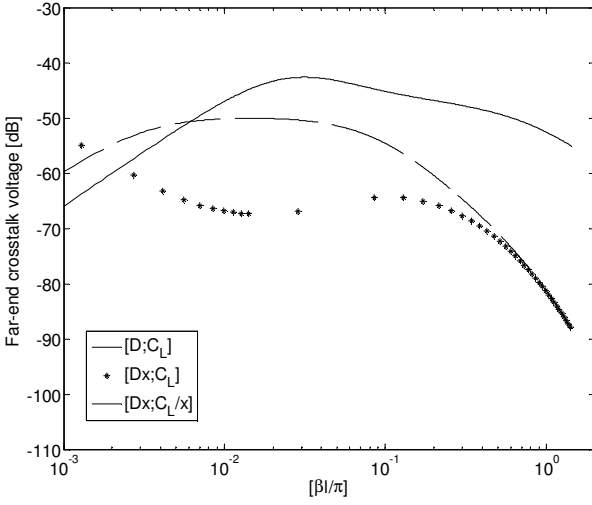


Figure 6. Far-end crosstalk noise for the circuit in Fig.5, assuming a nanoscale TL model (two CNT lines), after scaling the wire diameter D and/or the load capacitance C_L by a factor x .

As observed for the classical model, the reduction of the load capacitor shifts the peak of the noise to higher frequency values. The novelty is the sensitivity to the wire diameter that breaks the scaling rule observed in the classical solution. The reason is due to the impact of the number of conducting channels M on the kinetic inductance L_k and the quantum capacitance C_q (see (13)). For low values of M , L_k is usually larger than the magnetic inductance, hence the p.u.l. inductance matrix (which includes L_k only in the self terms) becomes diagonally dominant. This dominance depends on M , which in turns is related to the wire diameter and temperature [34-36]. In our case, at room temperature we pass from $M \approx 20$ (for multi-wall CNTs), to $M \approx 2$ (for single-wall CNTs). By increasing M , the bulk behavior is reached, while L_k and C_q become negligible. As pointed out in subsection II.A, this happens for single metallic NWs or bundles of thousands of CNTs, when diameter D reaches the values of hundreds of nm or greater. This is usually the case of practical applications of CNT on-chip interconnects, therefore the mentioned phenomena is not observed in the crosstalk analysis of such interconnects [47].

B. A pair of quantum devices in entangled states

We now discuss the case of two uncoupled lossless TLs, fed by two ideal voltage sources and terminated with a pair of quantum devices in entangled states, as schematically depicted in Fig.7. The lines are assumed to be identical, thus having the same wavenumber $\beta = \omega\sqrt{LC}$ and characteristic impedance $Z_C = \sqrt{L/C}$. The device is the pair of quantum dots (see Fig.2) assumed to be in the superradiant entangled state, so that (16) holds. As shown in Fig.7, the device may be represented by a simple π -type two-port, derived from (16), with the self and mutual admittance given by:

$$Y_s = Z_L^{-1}, \quad Y_m = -(2Z_L)^{-1}. \quad (21)$$

Note that the coupling element, Y_m , has a negative real part, without contradicting the thermodynamic equilibrium. As noted by Schrödinger [48], “The whole system can be less uncertain than either of its entangled parts”. It means, that the whole equivalent circuit is better specified than its elements. In our case, a negative resistance of circuit element means that there is a special type of energy transfer inside the system, different from the outside energy supply. It strongly contradicts the intuitive concepts of classic crosstalk, in which the electromagnetic coupling should be described only by passive elements [12-14], [46]. For these reasons, the considered system is not equal to a pair of coupled harmonic oscillators and has no analogs in classical electrodynamics.

To study the circuit in Fig.7, each line may be represented as a two-port network via the transmission matrix [46]:

$$\mathbf{T} = \begin{bmatrix} T_s & T_{12} \\ T_{21} & T_s \end{bmatrix}, \quad \begin{cases} T_s = \cos(\beta l) \\ T_{12} = -iZ_c \sin(\beta l) \\ T_{21} = -iZ_c^{-1} \sin(\beta l) \end{cases}. \quad (22)$$

As in Section III.A, we evaluate the coupling by studying the voltage on the load Z_L of line 2, when $U_1 = 1V$ and $U_2 = 0V$. By coupling these boundary conditions to line matrix (21), we obtain a simple expression for the far-end voltage:

$$V_{FE} = \frac{1}{2} \frac{T_{12}}{T_s(T_{12} - Z_L T_s)} = \frac{1}{2} \frac{\tan(\beta l)}{\sin(\beta l) - i \frac{Z_L}{Z_C} \cos(\beta l)}. \quad (23)$$

In the following we assume that each quantum device is made by the GaAs double quantum dot proposed in [49] as a qubit for quantum computing. We consider the following values for the parameters in (14)-(16): $a \approx 20$ nm, $\omega_0 \approx [1 \div 1.5] \cdot 10^{15}$ rad/s, $\gamma \approx 3 \cdot 10^{11}$ Hz and $\mu \approx 7.59\hbar$ [50].

The frequency behavior of the far-end voltage is plotted in Fig.8, with varying values of the *frequency of quantum transition* ω_0 . As a consequence of the entanglement, the active line is able to excite signals into the victim line even in absence of inter-line coupling. The spectrum plotted in Fig.8 shows a resonance for $\omega = \omega_0$, besides the classical resonances due to the transmission lines (for $\beta l = n\pi/2$).

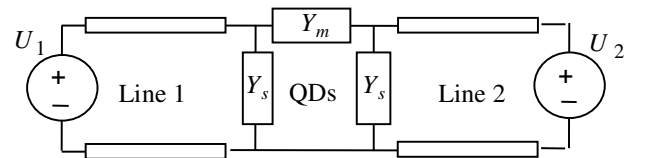


Figure 7. Equivalent scheme for the two uncoupled lines terminated on two coupled quantum devices, represented as a π -type two-port. The admittances are $Y_s = Z_L^{-1}$, $Y_m = -(2Z_L)^{-1}$, where Z_L is given by (14).

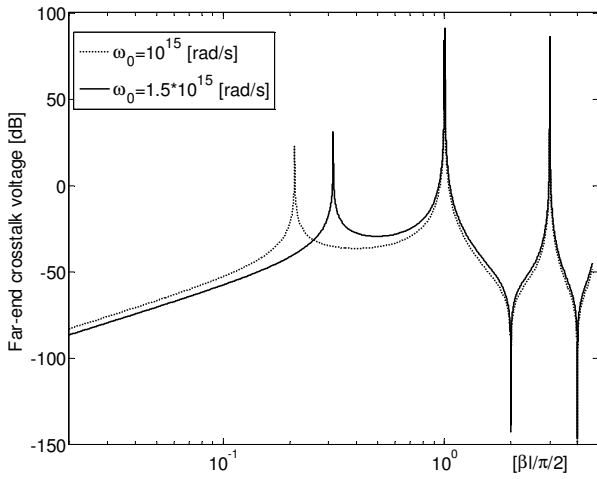


Figure 8. Far-end crosstalk voltage for coupled quantum loads, for different values of the quantum transition frequency.

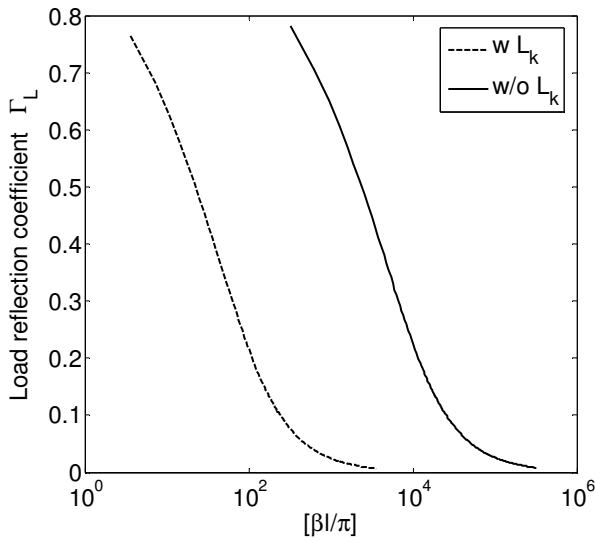


Figure 9. Load reflection coefficient for a lossy nano-transmission line, with or without the effect of the kinetic inductance.

C. Matching conditions

In this subsection we discuss the concept of matching, referring to a single transmission line made by one of the signal wires in Fig.1 and the ground plane. In the classical TL theory, the amplitude of the reflection coefficient at the load section is given by [46]:

$$\Gamma_L = \frac{1 - \zeta}{1 + \zeta}, \quad \zeta = \frac{Z_C}{Z_L}, \quad (24)$$

which leads to the classical *matching condition*

$$Z_L = Z_C, \quad (25)$$

giving $\Gamma_L = 0$. As it is well known, for a lossless line the characteristic impedance becomes a pure resistance

$Z_C = Z_{C0} = \sqrt{L/C}$, therefore a resistive load $Z_L = Z_{C0}$ would give a perfect matching at any frequency. For a lossy line the characteristic impedance become complex and frequency dependent: for instance, for the simple case of a lossy RLC line without skin-effect, it is:

$$Z_C(\omega) = \sqrt{\frac{R + i\omega L}{i\omega C}}. \quad (26)$$

It means that the load $Z_L = Z_{C0}$ would give a perfect matching condition only in the high frequency limit ($\omega \rightarrow \infty$).

If we consider the nanoscale TL, the situation qualitatively changes: the frequency range of satisfactory matching may be enlarged as a consequence of the presence of the kinetic inductance L_k . Let us consider, for instance, a metallic single-wall CNT with $D = 2\text{nm}$, $H = D$, and $l = 1\text{mm}$. In this case, $L_k/L_M \approx 1.3 \cdot 10^4$ and $C_E/C_q \ll 1$. Figure 9 plots the load reflection coefficient (24), evaluated with and without the contribution of L_k . If, for instance, in a given problem a satisfactory matching can be considered when the reflection coefficient less or equal to 0.1, then from Fig.9 is evident that in presence of kinetic inductance enlarges the region where this condition is fulfilled.

As shown for the crosstalk analysis, this effect vanishes when the number of channels M is large enough to lower the value of the kinetic term (for large diameter NWs or large CNT bundles).

Let us now discuss the concept of matching when an ideal TL is ended with a pair of quantum devices in the entangled state (see Fig.7). Assuming one of the two lines to be inactive, the reflection coefficient at the load of the other line may be expressed as:

$$\Gamma_L = e^{3i\beta l} \frac{2e^{-i\beta l} \cos(\beta l) - \zeta}{2e^{i\beta l} \cos(\beta l) + \zeta}, \quad \zeta = \frac{Z_C}{Z_L}, \quad (27)$$

which provides a new matching condition, that redefines (25):

$$Z_L = \frac{Z_C}{2} (1 + i \tan(\beta l)). \quad (28)$$

If we would impose the classical matching condition (25), we would obtain an energy reflection coefficient $[\Gamma_L]^2 \in [0.1, 1.0]$, depending on the phase shift βl . Condition (28) imposes an optimal phase shift between the source and the load in order to obtain total absorption, whereby the matching impedance becomes complex and depends on the line length. Thus, we obtain another result, important from EMC-point of view: quantum entanglement is able to break down the regime of matching between transmission line and the load.

IV. CONCLUSIONS

The new phenomena introduced by quantum effects in nano-electronic systems suggest a deep revision of the concepts adopted in the classical EMC analysis. The phenomenological approaches based on separable description of physical properties

of materials and electromagnetic response of electronic devices and systems become invalid on nanoscale. Instead, a self-consistent modeling of dynamics of quantum charge carriers and classical electromagnetic fields becomes necessary. The most efficient approach to this problem is based on the fundamental physical theory of generalized susceptibilities (Kubo-approach).

In this paper we have analyzed two case-studies: coupled nanoscale interconnects terminated with uncoupled loads, and coupled quantum devices in the entangled state connected to two uncoupled interconnects. In both cases, the coupling and matching conditions are dramatically modified, as compared to the classical EMC theory.

As for the nano-interconnects, their equivalent electrical parameters are affected by kinetic inductance and quantum capacitance, which introduce a new behavior with respect to the dimension scaling. The classical scaling rules no longer hold, as well as the separation rules adopted to mitigate the crosstalk. The kinetic inductance, however, plays a beneficial role, enlarging the attainable frequency range of the satisfactory matching of the load with the line.

A pair of quantum loads coupled via entanglement have been considered. As a result of quantum coupling, a voltage arises in the passive line, in spite of its electromagnetic decoupling with the active one. Thus, a novel concept arises: since the entanglement is a “spooky action at distance” his effects may surpass those due to the near field electromagnetic coupling, which are modeled by the cross-admittances. Quantum entanglement introduces a novel matching condition between the line and the load, with the optimal value of the load impedance dependent on the line length.

REFERENCES

- [1] M.A. Nielsen and I.L. Chuang, *Quantum Computation and Quantum Information*, Cambridge University Press, Cambridge, UK, 2010.
- [2] G.Ya. Slepyan, S.A. Maksimenko, V.P. Kalosha, J. Herrmann, N.N. Ledentsov, I.L. Krestnikov, Zh.I. Alferov, and D. Bimberg, “Polarization splitting of the gain band in quantum wire and quantum dot arrays”, *Phys. Rev. B*, vol. 59, pp. 1275-1278, 1999.
- [3] G.Ya. Slepyan, Y.D. Yerchak, A. Hoffmann and F.G. Bass, “Strong electron-photon coupling in a one-dimensional quantum-dot chain: Rabi waves and Rabi wave packets”, *Phys. Rev. B*, vol. 81, pp.085115 (1-18), 2010.
- [4] S.Iijima, “Helical microtubules of graphitic carbon,” *Nature*, vol. 354, pp. 56–58, 1991.
- [5] R. Van Noorden, “Moving towards a graphene world,” *Nature*, vol.442, no.7100, pp.228-229, Jul. 2006.
- [6] P. Avouris, Z. Chen, V. Perebeinos, “Carbon Based Electronics,” *Nature Nanotechnology*, vol. 2, no. 10, pp. 605, 2007.
- [7] A. H. Castro Neto, F. Guinea, N. M. R. Peres, K. S. Novoselov and A. K. Geim, “The electronic properties of graphene,” *Reviews of Modern Physics*, vol.81, pp.109-162, 2009.
- [8] J.-Y. Lee, S. T. Connor, Y. Cui, and P. Peumans, “Solution-Processed Metal Nanowire Mesh Transparent Electrodes,” *Nano Letters*, vol. 8, no.2, pp. 689-692, 2008.
- [9] L. Valitova, M. Amato, F. Mahvash, G. Cantele, A. Maffucci, C. Santato, R. Martel, and F. Ciccoira, “Carbon nanotube electrodes in organic transistors,” *Nanoscale*, vol. 5, pp. 4638-4646, 2013.
- [10] G.Ya. Slepyan, S.A. Maksimenko, A. Lakhtakia, O.M. Yevtushenko, and A.V.Gusakov, “Electrodynamics of carbon nanotubes: Dynamic conductivity, impedance boundary conditions and surface wave propagation”, *Phys. Rev. B*, vol. 60, pp. 17136-17149, 1999.
- [11] G. Ya. Slepyan, M. V. Shuba, S. A. Maksimenko, A. Lakhtakia, “Theory of optical scattering by achiral carbon nanotubes, and their potential as optical nanoantennas”, *Phys. Rev. B*, vol. 73, p.195416, 2006.
- [12] C. R. Paul, *Introduction to Electromagnetic Compatibility*, John Wiley & Sons, New York, 1992.
- [13] H.W. Ott, *Electromagnetic Compatibility Engineering*. John Wiley & Sons, New York, 2009.
- [14] M.I. Montrose, *EMC and the Printed Circuit Board*. IEEE Press, New York, 1999.
- [15] S. Datta, *Electronic Transport in Mesoscopic Systems*, Cambridge University Press. Cambridge, UK, 1995.
- [16] M. di Ventra, *Electrical Transport in Nanoscale Systems*, Cambridge University Press. Cambridge, UK, 2008
- [17] E.-P. Li, X.-C. Wei, A.C. Cangellaris, E.-X. Liu, Y.-J. Zhang, M. D’Amore, J. Kim, and T. Sudo, “Progress Review of Electromagnetic Compatibility Analysis Technologies for Packages, Printed Circuit Boards, and Novel Interconnects,” *IEEE Trans. on Electromagnetic Compatibility*, vol.52, no. 2, 248-265, May 2010.
- [18] M. D’Amore, M. S. Sarto, G. W. Hanson, A. Naeemi, and B. K. Tay, “Special Issue on Applications of Nanotechnology in Electromagnetic Compatibility (nano-EMC),” *IEEE Trans. on Electromagnetic Compatibility*, vol.54, no. 1, Feb. 2012.
- [19] V. Mordachev, E. Sinkevich, G. Slepyan, A. Boag, S. Maksimenko, P. Kuzhir, G. Miano, M. E. Portnoi, A. Maffucci, “Electromagnetic Compatibility Concepts at Nanoscale,” *Proc. of 2014 International symposium on Electromagnetic Compatibility*, EMC Japan 2014, Tokyo, Japan, pp.13-16, May 12-16, 2014.
- [20] F. Qin and C. Brosseau, “A review and analysis of microwave absorption in polymer composites filled with carbonaceous particles,” *J. Appl. Phys.*, vol. 111, pp. 061301–24, March 2012.
- [21] D.D.L. Chung, “Electromagnetic interference shielding effectiveness of carbon materials,” *Carbon*, vol.39, pp.279–85, 2001.
- [22] G. W. Hanson, “Fundamental transmitting properties of carbon nanotube antennas,” *IEEE Trans. Antennas and Propag.*, vol. 53, no. 11, pp. 3426–3435, Nov. 2005.
- [23] N. Li, Y. Huang, F. Du, X. He, X. Lin, H. Gao, Y. Ma, F. Li, Y. Chen , and P.C. Eklund, “Electromagnetic interference (EMI) shielding of single-walled carbon nanotube epoxy composites,” *Nano Letters*, vol.6, pp.1141-1145, 2006.
- [24] P.J. Burke, “An RF circuit model for carbon nanotubes,” *IEEE Trans. on Nanotechnology*, vol. 2, no. 1, pp.55-58, 2003.
- [25] A. Naeemi and J. D. Meindl, “Compact physical models for multiwall carbon-nanotube interconnects,” *IEEE Electron. Devices Lett.*, vol. 27, no. 5, pp. 338–340, May 2006
- [26] H. Li, C. Xu, N. Srivastava, and K. Banerjee, “Carbon Nanomaterials for Next-Generation Interconnects and Passives: Physics, Status, and Prospects,” *IEEE Trans. on Electron Devices*, vol.56, no.9, pp.1799-1821, 2009.
- [27] G. Antonini, A. Orlandi, L. Raimondo, “Advanced Models for Signal Integrity and Electromagnetic Compatibility-Oriented Analysis of Nanointerconnects,” *IEEE Trans. on Electromagnetic Compatibility*, vol.52, no. 2, pp.447-454, 2010.
- [28] G. Miano, C. Forestiere, A.Maffucci, S.A. Maksimenko and G. Ya. Slepyan, “Signal propagation in carbon nanotubes of arbitrary chirality”, *IEEE Trans. on Nanotechnology*, vol.10, no. 1, pp. 135-149, 2011.
- [29] C. Forestiere, A.Maffucci, S.A. Maksimenko, G.Miano and G. Ya. Slepyan, “Transmission-line model for multi-wall carbon nanotubes with intershell tunneling,” *IEEE Trans. on Nanotechnology*, vol.11, no. 3, pp. 554-564, 2012.
- [30] H. Zheng, Z. F. Wang, T. Luo, Q. W. Shi, J. Chen, “Analytical study of electronic structure in armchair graphene nanoribbons,” *Physical Review B*, vol. 75, p.165414, 2007.
- [31] Y. Zhou, S Sreekala, P M Ajayan and S K Nayak, “Resistance of copper nanowires and comparison with carbon nanotube bundles for interconnect applications using first principles calculations,” *J. Phys. Cond. Matter*, vol. 20, p.095209, 2008.
- [32] A. Maffucci, G. Miano, “A General Transmission Line Model for Conventional Metallic Nanowires and Innovative Carbon Nano-Interconnects,” *Proc. of IEEE Workshop on Signal and Power Integrity SPI 2013*, Paris, France, 12-15, pp.133-136, May 2013.
- [33] G. W. Hanson, “A Common Electromagnetic Framework for Carbon Nanotubes and Solid Nanowires—Spatially Dispersive Conductivity, Generalized Ohm’s Law, Distributed Impedance, and Transmission Line Model,” *IEEE Trans. Microwave Theory and Techniques*, vol. 59, pp.9-20, 2011.

- [34] C. Forestiere, A. Maffucci, G. Miano, "On the Evaluation of the Number of Conducting Channels in Multiwall Carbon Nanotubes," *IEEE Transactions on Nanotechnology*, vol.10, No.6, 1221-1223, 2011.
- [35] A. G. Chiariello, A. Maffucci, G. Miano, "Electrical Modeling of Carbon Nanotube Vias", *IEEE Transactions on Electromagnetic Compatibility*, vol.54, no.1, pp.158-166, Feb. 2012.
- [36] A. G. Chiariello, A. Maffucci, G. Miano, "Circuit Models of Carbon-based Interconnects for Nanopackaging, *IEEE Transactions on Components, Packaging and Manufacturing*, vol.3, no.11, pp.1926-1937, Nov. 2013.
- [37] A. A. Maarouf, C. L. Kane, and E. J. Mele. "Electronic structure of carbon nanotube ropes," *Physical Review B*, vol.61, pp.11156-11165, 2000.
- [38] T. D. Ladd, F. Jelezko, R. Laflamme, Y. Nakamura, C. Monroe, and J. L. O'Brien, "Quantum computers," *Nature*, vol.464, pp.45-53, Mar. 2010.
- [39] G.S. Agarwal, *Quantum Optics*, Cambridge University Press, Cambridge, UK, 2013.
- [40] G. Burkard, D. Loss, and D. P. Di Vincenzo, "Coupled quantum dots as quantum gates," *Phys. Rev. B*, vol. 59, pp.2070, 1999.
- [41] G. Shinkai, T. Hayashi, T. Ota, and T. Fujisawa, "Correlated Coherent Oscillations in Coupled Semiconductor Charge Qubits," *Phys. Rev. Lett.*, vol. 103, p.056802, 2009.
- [42] J.-J. Greffet, M. Laroche and F. Marquier, "Impedance of a Nanoantenna and a Single Quantum Emitter," *Phys. Rev. Lett.*, vol. 105, p.117701, 2010.
- [43] N. Engheta, A. Salandrino, and A. Alu, "Circuit Elements at Optical Frequencies: Nanoinductors, Nanocapacitors, and Nanoresistors" *Phys. Rev. Lett.*, vol. 95, p.095504, 2005.
- [44] L. D. Landau and E. M. Lifshitz, *Statistical Physics, Course of Theoretical Physics*, Pergamon Press, New York, 1980.
- [45] S.V. Gaponenko, *Introduction to nano-photonics*, Cambridge, University Press, Cambridge, UK, 2009.
- [46] C. R. Paul, *Analysis of Multiconductor Transmission Lines*, Wiley-IEEE Press, 2007.
- [47] S. N. Pu, W. Y. Yin, J. F. Mao, and Q. H. Liu: "Crosstalk Prediction of Single- and Double-Walled Carbon-Nanotube (SWCNT/DWCNT) Bundle Interconnects." *IEEE Trans. on Electron Devices*, vol.56, no.4, pp.560-568, Apr. 2009.
- [48] E. Schrödinger, "Die gegenwaertige Situation in der Quantenmechanik." *Naturwissenschaften*, vol. 23, pp.823-828, 1935.
- [49] V. Kornich, C. Kloeffel, and D. Loss, "Phonon-mediated decay of singlet-triplet qubits in double quantum dots", *Phys. Rev. B*, vol. 89, p.085410, 2014.
- [50] G. Ya. Slepyan, Y. D. Yerchak, A. Hoffmann, and F. G. Bass, "Strong electron-photon coupling in a one-dimensional quantum dot chain: Rabi waves and Rabi wave packets," *Physical Review B*, vol.81, p.085115, Feb. 2010.



Gregory Ya Slepyan received the M.S. degree in radioengineering from the Minsk Institute of Radioengineering, Minsk, Belarus, the Ph.D. degree in radiophysics from the Belarus State University (BSU), Minsk, and the Dr.Sci. degree in radiophysics from the Kharkov State University, Kharkov, Ukraine, in 1974, 1979, and 1988, respectively.

During 1992-2012, he was a Principal Researcher with the Laboratory of electrodynamics of nonhomogeneous media at the Institute for Nuclear Problems, BSU. Since 2013 he is a Professor-Resercher at the Department of Physical Electronics, School of Electrical Engineering, Tel Aviv University, Israel. He teaches courses on classical electrodynamics, nano-electromagnetism, metamaterials. He has authored or coauthored 2 books, 7 collective monographs, 130 journal articles. His current research interests include high-power microwave electronics, antennas and microwaves, diffraction theory, nonlinear waves, quantum optics and nanophotonics (including electrodynamics of graphene, carbon nanotubes and quantum dots).

Dr. Slepyan is a member of the Editorial Boards of the journals *Electromagnetics*, *Applied Sciences*.



Amir Boag (S'89-M'91-SM'96-F'08) received the B.Sc. degree in electrical engineering and the B.A. degree in physics in 1983, both Summa Cum Laude, the M.Sc. degree in electrical engineering in 1985, and the Ph.D. degree in electrical engineering in 1991, all from Technion - Israel Institute of Technology, Haifa, Israel.

From 1991 to 1992 he was on the Faculty of the Department of Electrical Engineering at the Technion. From 1992 to 1994 he has been a

Visiting Assistant Professor with the Electromagnetic Communication Laboratory of the Department of Electrical and Computer Engineering at the University of Illinois at Urbana-Champaign. In 1994, he joined Israel Aircraft Industries as a research engineer and became a manager of the Electromagnetics Department in 1997. Since 1999, he is with the Physical Electronics Department of the School of Electrical Engineering at Tel Aviv University, where he is currently a Professor.

Dr. Boag's interests are in computational electromagnetics, wave scattering, imaging, and design of antennas and optical devices. He has published over 95 journal articles and presented more than 200 conference papers on electromagnetics and acoustics. In 2008, Amir Boag was named a Fellow of the IEEE for his contributions to integral equation based analysis, design, and imaging techniques.



Vladimir Mordachev was born in Vitebsk, Belarus. He received the Ph.D. degree (1984), an academic rank of Senior Scientist (1985), and the M.S. degree with honors (1974) in Radio Engineering from the Minsk Radio Engineering Institute, Minsk, Belarus.

His research interests include spectrum management, wireless communications and networks, electromagnetic compatibility and interference, wireless

network planning, computer-aided analysis and design, cellular networks system ecology, RF systems modeling and simulation. He is extensively involved in consulting to wireless network operators, industry and the local government.

V. Mordachev is a head of the Electromagnetic Compatibility Laboratory at the Belorussian State University of Informatics and Radioelectronics.



Eugene Sinkevich (M'11) received the M.S. Degree in Radio System Engineering *summa cum laude* from the Belarusian State University of Informatics and Radioelectronics (BSUIR), Belarus, in 2000.

From 2000 to 2003, he was with the Department of Radio Engineering Theory, BSUIR. From 2004 to 2005, he was with the Department of Radio Devices, BSUIR. Since 2005, he is with the EMC R&D Lab., BSUIR, where he is currently Senior Researcher, team leader, and principal designer of international

R&D projects.

His research areas include electromagnetic compatibility, RF & microwave measurements, wireless systems and devices. He is author of about 20 technical papers on international journals and conference proceedings.



Polina Kuzhir received the M.D. degree in theoretical physics from Belarusian State University, Minsk, Belarus, in 1991, and the Ph.D. degree in high energy physics, in 1996 from the Institute of Physics, Belarus Academy of Science, Minsk.

She is currently a Senior Researcher at the Research Institute for Nuclear Problems, Belarus State University.

Her research interests include nano-electromagnetics. She is actively involved in experimental research of electromagnetic response of nanocarbon composite materials in microwave and terahertz ranges. She also contributes into investigation of electron beam instabilities in carbon nanotubes and graphene. She participates in several FP7 projects.



Sergey Maksimenko received the M.S. degree in physics of heat and mass transfer and Ph.D. degree in theoretical physics from Belarusian State University (BSU), Minsk, Belarus, in 1976 and 1988, respectively, and the Doctor of Science degree in theoretical physics from the Institute of Physics, Belarus National Academy of Science, Minsk, Belarus, in 1996. Since 1992, he was the head of laboratory at the Research Institute for Nuclear Problems, BSU, and since 2013 is the director this institute. His current research interests lie in fundamental and applied

nanoelectromagnetics and nanotechnology with focus on nanocarbon based radiation protective and shielding materials. He authored or co-authored more than 180 papers in international journals and conference proceedings, and book chapters. Prof. Maksimenko is a SPIE Fellow, associate editor of the Journal of Nanophotonics, co-chair of several international conferences. He was a coordinator of EU FP7 project FP7-226529 BY-NANOERA and currently is a leader of the Belarus team in the GRAPHENE FLAGSHIP project FP7-604391.



Giovanni Miano received the Laurea (*summa cum laude*) and Ph.D. degrees in electrical engineering from the University of Naples Federico II in 1983 and 1989, respectively.

From 1984 to 1985, he was with the PS Division, CERN, Geneva, Switzerland. From 1989, he is Full Professor at the faculty of Engineering of the University of Naples Federico II. From 2005 to 2009 he was the Director of the Dipartimento di Ingegneria Elettrica.

In 1996, he was a Visiting Scientist at the GSI Laboratories, Darmstadt, Germany, and in 1999 a Visiting Professor at the Department of Electrical Engineering, University of Maryland, College Park.

His research interests include ferromagnetic materials, nonlinear dielectrics, plasmas, electrodynamics of continuum media, nanotechnology and modeling of lumped and distributed circuits.

He is the author or coauthor of more than 70 papers published in international journals, 60 papers published in international conference proceedings, two items in the *Wiley Encyclopedia of Electrical and Electronic Engineering* (New York: Wiley, 1999), and the monograph *Transmission Lines and Lumped Circuits* (New York: Academic, 2001). He was member of the Editorial Boards of the Conference on Electromagnetic Field Computation and the Conference on the Computation of Electromagnetic Field.



Mikhail E. Portnoi is an Associate Professor of Physics at the University of Exeter, UK. He obtained his MSc degree in Electronics Engineering from the Leningrad Electrotechnical Institute in 1988, Candidate of Physical-Mathematical Sciences degree from the A.F. Ioffe Physico-Technical Institute of the Russian Academy of Sciences in 1994 and PhD in Physics from the University of Utah, USA, in 1996.

His research interests include carbon nanotubes, graphene, excitons and electron-hole plasma in semiconductor quantum wells, THz optoelectronics, optical spin orientation in semiconductors and the quantum Hall effect.

He is an author of over 200 journal and conference proceedings papers, three book chapters and a book. He serves as an Associate Editor of the SPIE Journal of Nanophotonics.



Antonio Maffucci (S'98-M'02-SM'11) received in 1996 the Laurea Degree in Electronic Engineering *summa cum laude* and in 2000 the Ph.D. degree in Electrical Engineering from the University of Naples "Federico II", Italy.

In 1997, he was with the nuclear fusion laboratory JET (Culham, U.K.). From 1998 to 2002, he was with the Department of Electrical Engineering, University of Naples Federico II. From 2002 he is with the Department of Electrical and Information Engineering at the University of Cassino and

Southern Lazio, where he is currently Associate Professor of Electrotechnics. His research areas include electromagnetic modeling, electromagnetic compatibility and nanotechnology. He is author of about 120 technical papers on international journals, conference proceedings and essays on books. He is also co-author of the book *Transmission lines and lumped circuits* (New York, Academic Press, 2001).

He is currently Associate Editor of the IEEE TRANSACTIONS ON COMPONENTS, PACKAGING, AND MANUFACTURING TECHNOLOGY and member of IEEE Nanopackaging Council.

He was the recipient of the Best paper award at IEEE Workshop on Signal Propagation on Interconnects 2009 and of the Outstanding Paper Award from "Literati Network Awards for Excellence 2008".